PROCEEDINGS OF SCIENCE

Detection of Supernova Remnants in the Large Magellanic Cloud at GeV Energies by Means of Cluster Analysis

A. Tramacere,[a,*] **R. Campana,**[b] **E. Massaro,**[c] **F. Bocchino,**[d] **M. Miceli**[d,e] **and S. Orlando**[d]

[a] *Department of Astronomy, University of Geneva, Chemin Pegasi 51, 1290, Versoix, Switzerland*
[b] *INAF/OAS, via Gobetti 101, 40129, Bologna, Italy*
[c] *INAF/IAPS, via del Fosso del Cavaliere 100, I-00113 Roma, Italy*
[d] *INAF/Osservatorio Astronomico di Palermo, Piazza del Parlamento 1, I-90134 Palermo, Italy*
[e] *Dipartimento di Fisica e Chimica E. Segrè, Università di Palermo, Piazza del Parlamento 1, 90134, Palermo, Italy*

E-mail: andrea.tramacere@unige.ch

We report the results of a new search using a 15-year long (up to August, 4 2023) *Fermi*-LAT data set at energies higher than 4 GeV for SNRs in the Large Magellanic Cloud applying two clustering methods: the Minimum Spanning Tree (MST), and the combination of Density-Based Spatial Clustering of Applications with Noise (DBSCAN) and DENsity-based CLUstEring (DENCLUE). We found positive indications for 8 new clusters with a spatial correspondence with SNRs, and increase the number of detected or candidate remnants in the high energy rays to 16 sources. These findings confirm the capability of clustering algorithms to extract local photon concentrations even in not uniform fields like the LMC and extend our knowledge on the relation between the X-ray and gamma-ray SNRs at low luminosities.

39th International Cosmic Ray Conference (ICRC2025)
15–24 July 2025
Geneva, Switzerland

ICRC 2025
The Astroparticle Physics Conference
Geneva July 15-24, 2025

[*]Speaker

© Copyright owned by the author(s) under the terms of the Creative Commons Attribution-NonCommercial-NoDerivatives 4.0 International License (CC BY-NC-ND 4.0).

PoS(ICRC2025)591

1. Introduction

The near irregular galaxy Large Magellanic Cloud (LMC) is particularly rich with supernova remnants (SNRs), whose ages span from about 40 years to a few tens of thousands of years.

The first observation of the LMC at energies higher than 100 MeV was made by [1] who used *Compton Gamma Ray Observatory* (CGRO) EGRET data. Abdo et al. (2010) [2] considered data *Fermi*-Large Area Telescope (*Fermi*-LAT; [3]) and discovered a bright, extended high-energy source related to the massive star-forming region 30 Doradus. A subsequent [4] analysis of the LMC region of *Fermi*-LAT data that span the first 6 years of the mission detected four point-like γ-ray sources. The DR4 (version v34) of the 4FGL catalog [5, 6] contains 18 sources detected in the 50 MeV – 1 TeV energy range, four of them reported as extended, and seven are in the 3FHL catalog [7] above 10 GeV. Nine other 4FGL sources are background extragalactic counterparts (indicated as unclassified blazar or BL Lac objects). The H.E.S.S. collaboration observed three sources up to about 10 TeV in the LMC [8]: two of them associated with the SNRs N 157B [9] and N 132D. The former contains the highest known spin-down luminosity pulsar, PSR J0537−6910 [10, 11], with a period of 16 ms.

Campana et al. (2018) [12] (Paper I) used *Fermi*-LAT data collected in 9 years for a photon cluster search above 10 GeV and discovered the high-energy emission from the two SNRs N 49B and N 63A. Campana et al. (2022) [13] (Paper II), applied the cluster search to *Fermi*-LAT data over 12 years with energy higher than 6 and 10 GeV. Previous detections were confirmed, and a couple of clusters associated with the SNRs N49 and N44 were found. Another cluster likely, associated with N186D, was detected at energies higher than 6 GeV.

In the present contribution, we used a dataset of 15 years of *Fermi*-LAT observation and energies higher than 4 GeV. As in Paper II, we apply the two cluster-finding methods density-based spatial clustering of applications with noise (DBSCAN) [14], and the minimum spanning tree (MST; see [15, 16]) to extract spatial concentrations of photons tracing genuine γ-ray sources. In particular, the DBSCAN algorithm has been coupled to the DENsity-based CLUstEring (DENCLUE) algorithm [17], to improve the study of confused sources. The results of this new analysis confirm the previous SNR detections with a higher significance, and sorted other photon clusters at positions very close to SNRs not previously associated with γ-ray emitters. A more detailed account can be found in the recent paper [18]

2. Data selection in the LMC region

We analyzed *Fermi*-LAT data collected from August 4, 2008, to August 4, 2023, including events above 4 GeV. The complete dataset was retrieved as weekly files from the Fermi Science Support Center archive.[1] The dataset was processed using the Pass 8, release 3, reconstruction algorithm and includes the instrumental responses. The event lists were filtered by applying the standard selection criteria on data quality and zenith angle (source class events, `evclass` 128), front and back converting (`evtype` 3), up to a maximum zenith angle of 90°. Events were then screened for standard good time interval selection. We selected a region $12^\circ \times 9^\circ$ in Galactic coordinates $271^\circ < l < 287^\circ$ and $-38^\circ < b < -29^\circ$, centered at the LMC and including the whole galaxy.

[1] http://fermi.gsfc.nasa.gov/ssc/data/access/

PoS(ICRC2025)591

Table 1: Supernova remnants already detected at energies higher than 4 and 10 GeV and confirmed by the present analysis.

SNR	RANGE GeV	TYPE	D ′	L_X	$S_{\rm cls}4$	$S_{\rm cls}10$	Δ ′	N/M 4 GeV	N/M 10 GeV
N 44	>4;10	–	4.3	0.90	4.8	3.3	3.7	26/48.1	13/28.7
N 132D	>4;10	CC	2.1	315.04	6.6	4.6	1.8	27/55.6	21/57.6
N 49B	>4*;10	CC	2.8	38.03	*5.6	*3.9	3.4	*23/46.3	6/20.0
N 49	>4*;10	CC-SGR	1.4	64.37	*5.6	*3.9	3.5	*23/46.3	9/18.4
B0528−692	>10		4.5	1.99	4.4	3.5	4.1	24/55.7	24/58.8
N 63A	>4;10	CC	1.4	185.68	6.5	4.1	0.4	33/92.9	15/53.7
N 157B	>4;10	CC-PWN	2.0	15.00	18.8	11.6	1.6	146/441.5	155/577.4
B0540−693	>10	CC-PSR	1.2	87.35	8.7	4.8	5.3	22/61.8	8/35.4
N 186D	>4;6		1.9	1.09	—	3.7		9/17.1	7/19.0

Angular separations are from MST; X-ray luminosities is in units of 10^{35} erg/s. * : Unresolved cluster at energies lower than 10 GeV; D: SNR diameter; Δ: Angular separation; L_X: X-ray luminosity in the band 0.3–8 keV from the Maggi et al. (2016) catalog; $S_{\rm cls}$: Significance of the DBSCAN clusters above 4 and 10 GeV; N; M: Number of photons in the clusters and magnitude from MST.

Given the condition of a high local diffuse emission in the LMC, the sorting of point-like sources is a quite delicate work. Our basic choice was to search clusters above 10 GeV since the diffuse component is rather weak in this band. Once a list of clusters was obtained, we searched for correspondent features at lower energies, and if they were found, the cluster was considered to be confirmed. We also used smaller fields not including the 30 Dor nebula because its relatively high number of photons produces a too short mean angular separation. Analyses at lower energies generally imply that the resulting “cluster parameters" are generally lower than above 10 GeV, and the extraction of clusters is less stable, that is small changes in the selection parameters could yield different structures. The catalog of Maggi et al. (2016) [19] reports 59 remnants. A new complete catalog (hereafter ZMC24) has been recently published by [20]. It is based on the eROSITA X-ray survey and includes 78 entries. We did not find any positional correspondence between clusters and the new additions of ZMC24 to the list of Maggi et al.[19]. Therefore, we limited our analysis to the latter sample, which contains all the brightest SNRs.

3. Clustering algorithms for photon cluster detection

We applied the DBSCAN-DENCLUE algorithm uses the local density of points to find clusters in datasets affected by background noise (for a detailed description, see [14, 18]). The DBSCAN builds the cluster by recursively connecting “density connected" points to each set of “core" points found in a set of photons where each element is described by the sky coordinates. Each cluster C_m is described by the position of the centroid (x_c,y_c), the ellipse of the cluster containment, the number of photons in the cluster (N_p), and the significance evaluated according to the signal-to-noise likelihood ratio test (LRT) method [21]. To deblend two (or more) “confused" sources, we used the DENCLUE algorithm [22, 23]. Notably, DENCLUE relies on kernel density estimation, defining clusters according to the local maxima of an estimated density function (see Tramacere et al. 2016 [17]).

PoS(ICRC2025)591

Table 2: New SNRs detected at energies higher than 4 GeV.

SNR	l deg	b deg	TYPE	D $'$	L_X	$S_{\rm cls}4$	Δ $'$	MST N/M	
B0453−685	279.793	−35.765	CC	2.0	13.85	3.7	2.0	10/18.3	
B0532−675	277.638	−32.346		4.7	2.48	3.1	5.8	7/23.5	e
[HP99]1139	281.589	−34.229		4.4	1.44	3.1	6.4	13/24.7	e
N 103B	279.624	−34.401	Ia	0.5	51.70	3.3	2.7	10/19.8	
B0519−690	279.617	−33.323	Ia	0.6	34.94	4.2	5.0	13/26.6	
DEM L316A/B	279.984	−30.859	Ia/CC	3.2	1.47/1.26	4.7	4.1	11/21.5	Nf
DEM L241	277.712	−32.150		5.3	3.84	5.2	1.2	35/79.6	

Coordinates and angular separations are from MST; X-ray luminosities is in units of 10^{35} erg/s. e: MST analysis at energies >6 GeV; Nf: M value obtained in a field with $b > -31°$; $S_{\rm cls}$: Significance of the DBSCAN clusters above 4 GeV; N, M: Number of photons in the clusters and magnitude from MST.

The other method is based on the MST algorithm which searches spatial concentrations in a field of points (see, for instance, [25] and also [15, 16]). The application of this method to the γ-ray sky and selection criteria have been presented elsewhere (e.g., in [12]). Once computed the graph without closed loops connecting all the points with the minimum total distance, we selected clusters by eliminating all the edges having a length higher than a threshold and a number of nodes higher than a fixed minimum value. For each residual subset we evaluated a very useful parameter M, the *cluster magnitude*, defined as the product of the photon number and of the ratio between the mean distance in the total tree divided by that in the cluster. The square root was found well correlated with other statistical source significance parameters [16].

4. Results of cluster analysis at energies above 4 and 10 GeV

As reported in Table 1, all clusters in Paper II are safely confirmed by both methods, and the DBSCAN/DENCLUE significance was higher than 3 standard deviations for all sources in the two considered energy ranges, with the exception of the two very close and unresolved SNRs N 49 and N 49B. The detection of the SNR N 186D is confirmed by DBSCAN/DENCLUE at energies higher than 10 GeV, whereas MST gives a cluster with the same number of photons as in Paper II but a slightly lower M due to the higher mean photon density.

The search for photon clusters above 4 GeV is more difficult because of the large increase of the background and a broader PSF both implying a consequent decrease in the density contrast. We note that the values of the magnitude M are generally higher than 20, the threshold adopted above 10 GeV. Only two clusters in Table 2 have a M values lower than 20: one has $M = 19.8$ and the other has 18.3, which are slightly lower the threshold and marginally acceptable at these energies.

We also performed a new MST analysis in a region with the boundaries $l \in (274; 281)$ and $b \in (-40; -33)$, thus excluding the bright 30 Dor complex, that confirmed the clusters corresponding to the powerful SNRs with the same numbers of photons but with slightly higher magnitudes, namely: $M = 20.2$ for B0453−685, $M = 21.8$ for N103B, and $M = 29.4$ for B0519−690.

PoS(ICRC2025)591

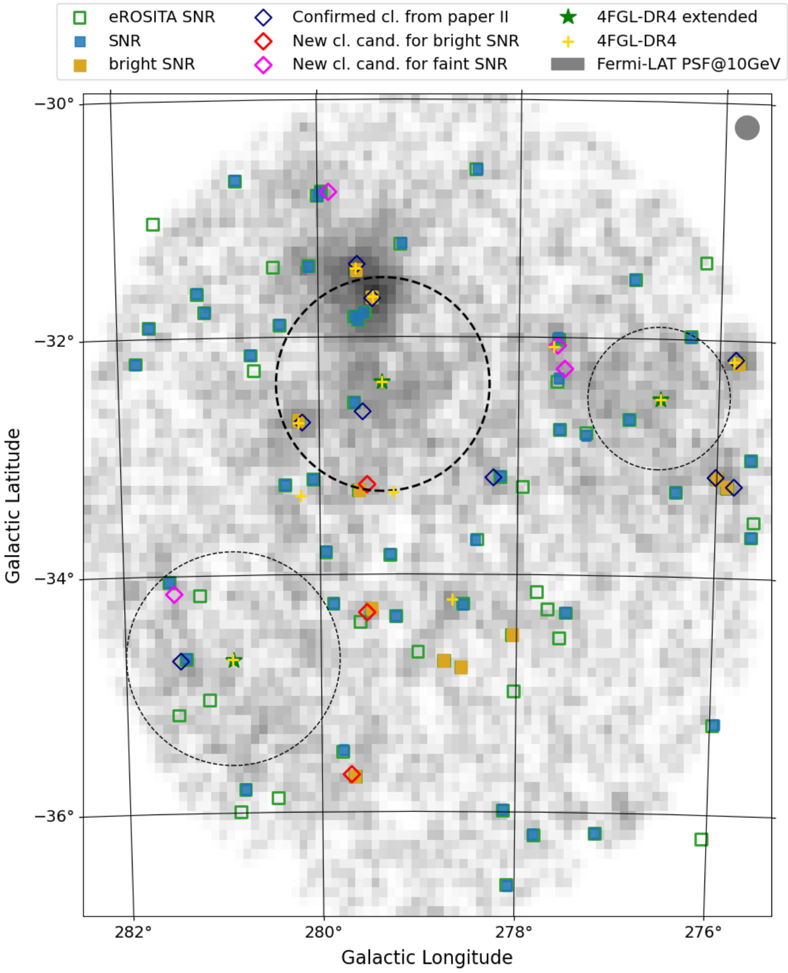

Figure 1: Map of the region of the LMC reporting the known SNRs, 4FGL-DR4 sources, and the photon clusters found in the present work. Solid squares identify SNRs from [19]. Green empty squares identify SNRs from [20]. Blue diamonds are confirmed clusters form [24], and red and purple diamonds are clusters detected in the present analysis for bright and faint SNRs, respectively. Yellow crosses mark 4FGL-DR4 point-like sources, dashed circles represent the approximate size of the extended 4FGL sources, the thick circle is that containing the 30 Dor complex, and green stars mark their centers.

The cluster likely associated with [HP99]1139 was found above 6 GeV but not above 4 GeV, and the one associated with the complex DEM L316A/B was not found in the very large field, whereas a positive detection resulted in a narrow field excluding the bright region of 30 Dor. We also searched in the primary selection list of clusters above 10 GeV for entries corresponding to these remnants, and found only a low-significance cluster at the position of DEM L241, whose photon number is the highest.

In Figure 1, a map of the LMC is shown with the locations of the clusters. The new ones are outside the very bright region of 30 Dor, and the four clusters associated with faint SNRs are at distances greater than 1 degree from the external boundary. The other three clusters in Table 2 (i.e., B0453−685, N 103B, and B0519−690) are in the subsample of bright X-ray emitters undetected in Paper II, and therefore they could be considered as best candidates. The first of them was already

PoS(ICRC2025)591

detected by [26], while the other two are new findings.

The peculiar object DEM L316A/B, appears to be composed of two overlapping remnants (indicated by the letters A and B) and was investigated in the radio and optical by [27]. However, the possibility that the two remnants are actually interacting has not been confirmed by X-ray data analyses [28, 29]. The two remnants are different in size, but both have rather large diameters ($2'$and $3'$, corresponding to about 30 and 40 pc) and are relatively evolved, with estimated ages of 27 kyr and 39 kyr. The centroid coordinates of the cluster given in Table 2 are closer to the remnant A, but both these objects can contribute to the photon cluster because its maximum radius is equal to $6'.7$ and the angular distance between the centers of the remnants is around only $2'.4$, lower than the instrumental PSF at 4 GeV.

The source P3 in [4] was unassociated since DEM L241 and other possible counterparts, were distant from the best-fit position. Its spectrum was found to be quite soft, with an estimated photon index equal to 2.8. The corresponding source 4FGL J0535.2-6736, is at a distance of about $5'$ from the remnant, and the counterpart is a HMXB because its γ-ray flux exhibits a modulation with a period of 10.3 days, the same as the HMXB [30].

At energies higher than 4 GeV, the present analysis provides a very significant cluster either with DBSCAN or DENCLUE and with MST (25 photons, $M = 56.67$) at a position fully consistent with the known source and the SNR, while MST selection sample above 10 GeV gives a poorly significant cluster at (83.8996, −67.5959) with five photons and $M = 9.6$, which could be consistent with a soft spectral distribution. If high-energy photons are mostly emitted by the HMXB rather than the remnantthis source cannot be included in the sample of genuine γ-ray loud SNR.

5. Conclusions

This analysis exploiting 15 years of *Fermi*-LAT observations confirms that the LMC region exhibits a significant clumpy structure in the γ-ray emission and has several photon clusters closely associated with SNRs. The number of γ-ray-detected SNRs in the LMC above 4 GeV is now increased to 15 and represents approximately 25% of the Maggi et al. sample, or 19% of the ZMC24 catalog. The results of our cluster analyses of the photon field of the LMC region can be summarized as follows:

- We detected photon clusters whose centroids are at angular separations of only a few arcminutes from 15 SNRs. More specifically, eight SNRs were found above 10 GeV and one above 6 GeV. The other six remnants are above 4 GeV.
- One of these clusters corresponds to a very close pair of SNRs (DEM L316A and DEM L316B) that have a separation smaller than the PSF diameter, and therefore their γ-ray emission cannot be resolved.
- There is robust evidence for a cluster corresponding to the SNR DEM L241, a source already detected and exhibiting a clear modulation with the period of an X-ray binary inside the remnant.
- We also searched for clusters close to the position of the very young SNR 1987A but did not find any significant feature. This source, however, is close to the bright region of 30 Dor, and the local high spatial density of photons makes cluster extraction quite difficult.

PoS(ICRC2025)591

- The remnants previously reported in Paper II were all of the CC type, while in the present analysis we also found two Ia SNRs, although only at energies higher than 4 GeV. Their emission, therefore, appears generally softer than CC remnants.

However, some challenges remain: (*i*) Three SNRs in the bright subsample (B0509−67.5, DEM L71, and N 23) are not associated with significant γ-ray clusters despite expectations of detectable emission; (*ii*) Six low-luminosity SNRs are detected in γ-rays with different degrees of significance, while several other sources of comparable luminosity remain undetected. Given the proximity, the low metallicity and intense star formation history, the LMC provides a unique laboratory with conditions similar to those of primeval galaxies in the early Universe. Our findings are therefore useful to refine the understanding of young SNR evolution, particle acceleration, and progenitor-type differences.

References

[1] P. Sreekumar, D.L. Bertsch, B.L. Dingus, C.E. Fichtel, R.C. Hartman, S.D. Hunter et al.*ApJ* **400** (1992) L67.

[2] A.A. Abdo, M. Ackermann, M. Ajello, W.B. Atwood, L. Baldini, J. Ballet et al. *A&A* **512** (2010) A7 [1001.3298].

[3] M. Ackermann, M. Ajello, A. Albert, A. Allafort, W.B. Atwood, M. Axelsson et al. *ApJS* **203** (2012) 4.

[4] M. Ackermann, A. Albert, W.B. Atwood, L. Baldini, J. Ballet, G. Barbiellini et al. *A&A* **586** (2016) A71.

[5] S. Abdollahi, F. Acero, M. Ackermann, M. Ajello, W.B. Atwood, M. Axelsson et al. *ApJS* **247** (2020) 33 [1902.10045].

[6] J. Ballet, T.H. Burnett, S.W. Digel and B. Lott*arXiv e-prints* (2020) arXiv:2005.11208 [2005.11208].

[7] M. Ajello, W.B. Atwood, L. Baldini, J. Ballet, G. Barbiellini, D. Bastieri et al. *ApJS* **232** (2017) 18 [1702.00664].

[8] H.E.S.S. Collaboration, A. Abramowski, F. Aharonian, F. Ait Benkhali, A.G. Akhperjanian, E.O. Angüner et al.*Science* **347** (2015) 406.

[9] H.E.S.S. Collaboration, A. Abramowski, F. Acero, F. Aharonian, A.G. Akhperjanian, G. Anton et al. *A&A* **545** (2012) L2.

[10] F.E. Marshall, E.V. Gotthelf, W. Zhang, J. Middleditch and Q.D. Wang*ApJ* **499** (1998) L179.

[11] G. Cusumano, M.C. Maccarone, T. Mineo, B. Sacco, E. Massaro, R. Bandiera et al. *A&A* **333** (1998) L55.

[12] R. Campana, E. Massaro and E. Bernieri *Ap&SS* **363** (2018) 144 [1806.02040].

PoS(ICRC2025)591

[13] R. Campana, E. Massaro, F. Bocchino, M. Miceli, S. Orlando and A. Tramacere *MNRAS* **515** (2022) 1676 [2207.01272].

[14] A. Tramacere and C. Vecchio*Astronomy and Astrophysics* **549** (2013) A138.

[15] R. Campana, E. Massaro, D. Gasparrini, S. Cutini and A. Tramacere *MNRAS* **383** (2008) 1166.

[16] R. Campana, E. Bernieri, E. Massaro, F. Tinebra and G. Tosti *Ap&SS* **347** (2013) 169.

[17] A. Tramacere, D. Paraficz, P. Dubath, J.P. Kneib and F. Courbin *MNRAS* **463** (2016) 2939 [1609.06728].

[18] A. Tramacere, R. Campana, E. Massaro, F. Bocchino, M. Miceli and S. Orlando *A&A* **697** (2025) A200 [2503.20351].

[19] P. Maggi, F. Haberl, P.J. Kavanagh, M. Sasaki, L.M. Bozzetto, M.D. Filipović et al. *A&A* **585** (2016) A162.

[20] F. Zangrandi, K. Jurk, M. Sasaki, J. Knies, M.D. Filipović, F. Haberl et al. *A&A* **692** (2024) A237 [2401.17307].

[21] T.P. Li and Y.Q. Ma *ApJ* **272** (1983) 317.

[22] A. Hinneburg and D.A. Keim in *Proceedings of the Fourth International Conference on Knowledge Discovery and Data Mining*, KDD'98, p. 58–65, AAAI Press, 1998.

[23] A. Hinneburg and H.-H. Gabriel in *Proceedings of the 7th International Conference on Intelligent Data Analysis*, IDA'07, (Berlin, Heidelberg), p. 70–80, Springer-Verlag, 2007.

[24] R. Campana, E. Massaro and E. Bernieri *Ap&SS* **361** (2016) 183.

[25] T. Cormen, C. Leiserson, R. Rivest and C. Stein, *Introduction to Algorithms*, MIT Press, Cambridge, USA, 3rd ed. (2009).

[26] J. Eagle, D. Castro, P. Mahhov, J. Gelfand, M. Kerr, P. Slane et al. *ApJ* **945** (2023) 4 [2302.01836].

[27] R.M. Williams, Y.-H. Chu, J.R. Dickel, R. Beyer, R. Petre, R.C. Smith et al. *ApJ* **480** (1997) 618.

[28] R.M. Williams and Y.H. Chu *ApJ* **635** (2005) 1077 [astro-ph/0509696].

[29] J.C. Toledo-Roy, P.F. Velázquez, F. de Colle, R.F. González, E.M. Reynoso, S.E. Kurtz et al. *MNRAS* **395** (2009) 351.

[30] R.H.D. Corbet, L. Chomiuk, M.J. Coe, J.B. Coley, G. Dubus, P.G. Edwards et al. *ApJ* **829** (2016) 105.

PoS(ICRC2025)591